Suppression of Photon-Echo As a Signature of Chaos†

Maksym Kryvohuz and Jianshu Cao*

Department of Chemistry, Massachusetts Institute of Technology, Cambridge, Massachusetts 02139

Shaul Mukamel

Department of Chemistry, University of California, Irvine, California 92697-2025

Received: May 24, 2008; Revised Manuscript Received: August 7, 2008

The paper discusses the effect of quantum chaos on photon-echo signals of two-electronic-state molecular systems. The temporal profile of photon-echo signals is shown to reveal key information about nuclear dynamics on the excited electronic state surface. Specifically, the suppression of echo signals at a particular value of the delay time τ_1 between the first and second excitation pulses is demonstrated as a signature of quantum level statistics that corresponds to the classically chaotic nuclear motion in the excited electronic state surface.

I. Introduction

A great deal of theoretical work has been devoted to studying the signatures of chaos in quantum systems.[1−8] It has been shown that systems with regular dynamics have a Poisson distribution of energy level spacings, while systems with chaotic dynamics have level statistics similar to that of the Gaussian orthogonal ensemble (GOE) of random matrices. Obtaining level statistics from an experimental spectrum has practical difficulties;[9−11] thus, it is interesting to find effects of different level statistics on time domain signals, that is, quantum signatures of chaos in the time domain. Time domain experiments provide an opportunity to find the signatures of chaos without the necessity of resolving level statistics. In the present paper, we propose a photon-echo experiment which reveals an information on level statistics from a time domain echo signal.

Although the literature on the universal level statistics in strongly chaotic systems is controversial, the basic property of quantum chaos is the existence of energy level repulsion. One can think of level repulsion as being the result of the interaction between the "good quantum numbers" when the system changes its dynamics from regular to chaotic. For the Sinai billiard, which is a strongly ergodic classical system, it has been shown that its spectral fluctuations are similar to that of a random matrix of the Gaussian orthogonal ensemble.[12] It is assumed that the same result remains valid for all chaotic systems. For the convenience of analytical derivations, we assume GOE statistics of eigenstates with classically chaotic dynamics in the present paper. Yet, in section IV, we show that any form of spectral correlation can be used to obtain the information about spectral fluctuations from the time domain photon-echo signal.

The dynamics (either regular or chaotic) that underlies particular energy level statistics is of interest to chemical physicists. In the present paper, we consider a model of a polyatomic molecule with two electronic states. Nuclear energy levels of the excited electronic state obey either Poisson or GOE nearest-neighbor statistics, corresponding to regular or chaotic dynamics, respectively. Nuclear dynamics of multidimensional motion on the ground electronic potential energy surface is assumed to be quasi-periodic with Poisson statistics of nuclear levels. Poisson statistics of vibrational energy levels in the ground electronic state was observed in a lower energy range, for instance, for the molecule of N_2O.[13] In general, two independent anharmonic spectra can be sufficient to form a Poisson statistics.

The basic idea in searching for a time- domain signature of level statistics lies in averaging over the ensemble of time-dependent superposition states. Consider a quantum state $|\psi\rangle$, which is a superposition of two eigenstates $|n_1\rangle$ and $|n_2\rangle$ that correspond to eigenvalues E_{n_1} and E_{n_2}, respectively; then, after coherent excitation of $|\psi\rangle$, it will dephase due to the factor $\exp\{i(E_{n_1} - E_{n_2})t/\hbar\}$. The average over an ensemble of states $|\psi(t)\rangle$ in some cases is equivalent to the average over level spacings $E_{n_1} - E_{n_2}$, resulting in different time domain signals (because of the connection of time and level spacings in $\exp\{i(E_{n_1} - E_{n_2})t/\hbar\}$) for different level spacing statistics. Pechukas was the first to propose the idea that the average survival probability $P(t) = |\langle\psi(0)|\psi(t)\rangle|^2$ behaves differently for systems with chaotic and regular dynamics.[14] This idea was further developed by Wilkie and Brumer[15,16] to show that the time-resolved fluorescence depends on the average survival probability and therefore carries signatures of quantum chaos. Yet, information from a fluorescence experiment is hidden behind a fluorescence decay due to radiative damping. In the present paper, we propose another type of optical experiment, a nonlinear photon-echo experiment, and show that it can avoid the effects of dephasing and reveal the necessary information about level statistics. A photon-echo technique is well-known for its capability to remove the effects of inhomogeneous line broadening. Homogeneous line broadening effects cannot be removed in a photon-echo experiment, resulting in a signal decay that hides the necessary information contained in the signal's temporal profile, similarly to the fluorescence experiment. However, a nonlinear photon-echo experiment is an ultrafast experiment and allows one to resolve much smaller time scales than the fluorescence experiment discussed in ref 15. In this paper, we show that level statistics from a photon-echo experiment yields a universal time scale 4τ, where τ is a duration of the laser pulse. Given with the average signal decay rate $\bar{\Gamma}$ due to homogeneous line broadening mechanisms, one can always pick a laser pulse that will satisfy $\tau \ll 1/\bar{\Gamma}$ and thus

† Part of the "Karl Freed Festschrift".

* To whom correspondence should be addressed.

10.1021/jp804604h CCC: $40.75
Published on Web 11/13/2008

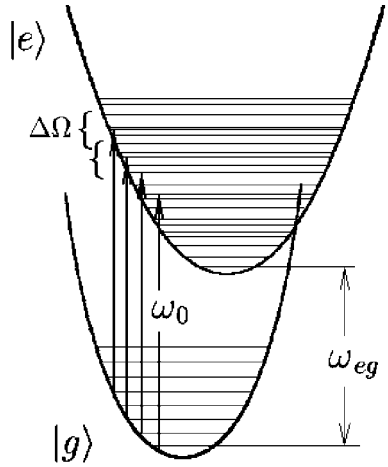

Figure 1. The molecular level scheme for a two-level system.

obtain *clean* information about the signal at time 4τ, which is not possible in the fluorescence experiment.

Consideration of a nonlinear experiment to extract information about chaos is also interesting in the context of recent studies of the effect of chaos in classical response theory. It was suggested by Mukamel and co-workers[17] that classical nonlinear response functions are good indicators of chaotic dynamics since stability matrices diverge linearly in time[18−22] for systems with quasi-periodic dynamics and exponentially for systems with chaotic dynamics. Chernyak and co-workers have recently shown[23,24] that classical nonlinear response functions exhibit frequency domain signatures of chaotic motions.

The present paper is organized as follows. In section II, we describe the nonlinear experiment and analytically derive the expression for the third-order polarization. In section III, we consider the differences in a photon-echo signal for systems with regular and irregular dynamics. In section IV, we discuss the effects of impurities of the spectral level statistics on the photon-echo signal. In section V, we discuss the suppression of the photon-echo signal at time $\tau_1 = 4\tau$ for chaotic systems.

II. Theory Section

We consider a system with two electronic states, ground $|g\rangle$ and excited $|e\rangle$. The adiabatic Hamiltonian of the system is given by

$$H = |g\rangle H_g\langle g| + |e\rangle(H_e + \omega_{eg})\langle e| \quad (1)$$

where H_g is the nuclear Hamiltonian on the ground electronic potential surface, H_e is the nuclear Hamiltonian on the excited electronic potential surface, and ω_{eg} is the electronic gap between the minima of both potentials (Figure 1). The nuclear dynamics of interest (either regular or chaotic) corresponds to Hamiltonian H_e, and thus, the statistics of nuclear energy levels in the excited electronic state is assumed to be either random (Poisson ensemble) or correlated (Gaussian orthogonal ensemble). Physically, only particular areas of the energy level spectrum of H_e obey particular level statistics; at low energies, nuclear dynamics is mostly quasiperiodic, and thus, the corresponding level statistics should be that of the Poisson ensemble, while at high energies, it can be chaotic with the corresponding statistics of the GOE. By changing the carrier frequency of the excitation pulse, we can select the energy region of interest.

The most common technique in nonlinear spectroscopy is a three-pulse photon-echo experiment. In this experiment, a system

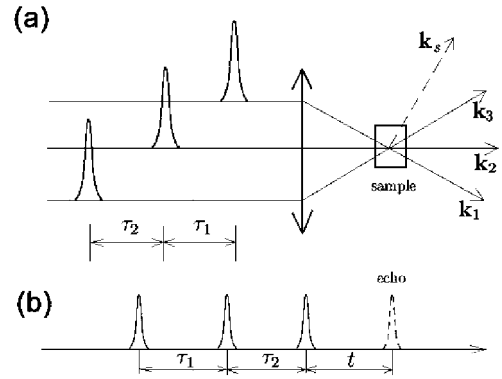

Figure 2. Three-pulse photon-echo experiment depicted in (a) space and (b) time.[25]

is irradiated with three subsequent pulses with delay periods of τ_1 and τ_2 between them. The measurement is done at time t after the third pulse (Figure 2). The electric field acting on a system is

$$E(\mathbf{r}, t) = E_1(t + \tau_2 + \tau_1)\exp(i\mathbf{k}_1\mathbf{r} - i\omega_1 t) + E_2(t + \tau_2)\exp(i\mathbf{k}_2\mathbf{r} - i\omega_2 t) + E_3(t)\exp(i\mathbf{k}_3\mathbf{r} - i\omega_3 t) \quad (2)$$

where ω_j and $\mathbf{k}_j$ are frequencies and wave vectors of the incident waves and $E_j(t)$ denotes the temporal envelope. We assume that all three pulses have the same frequencies $\omega_1 = \omega_2 = \omega_3 = \omega_0$ and temporal envelopes $E(t) = E_0 \exp(-t^2/2\tau^2)$, although they have different wavevectors $\mathbf{k}_j$. The photon-echo signal is measured in the direction $\mathbf{k}_s = \mathbf{k}_3 + \mathbf{k}_2 - \mathbf{k}_1$.[25] The corresponding nonlinear polarization is given by[25]

$$P^{(3)}(\mathbf{k}_s = \mathbf{k}_3 + \mathbf{k}_2 - \mathbf{k}_1, t) = \left(\frac{i}{\hbar}\right)^3 \int_0^\infty dt_3 \int_0^\infty dt_2 \int_0^\infty dt_1 [R_2(t_3, t_2, t_1) + R_3(t_3, t_2, t_1)] \times E_3(t - t_3)E_2(t + \tau_2 - t_3 - t_2)E_1^*(t + \tau_1 + \tau_2 - t_3 - t_2 - t_1) \times \exp[i(\omega_0 - \omega_{eg})(t_3 - t_1)] \quad (3)$$

where the two response terms in the photon-echo signal are

$$R_2(t_3, t_2, t_1) = \left\langle \hat{\mu} \exp\left[\frac{i}{\hbar}H_e(t_1 + t_2)\right]\hat{\mu} \exp\left[\frac{i}{\hbar}H_g t_3\right]\hat{\mu} \times \exp\left[-\frac{i}{\hbar}H_e(t_2 + t_3)\right]\hat{\mu} \exp\left[-\frac{i}{\hbar}H_g t_1\right]\rho_g \right\rangle \quad (4)$$

$$R_3(t_3, t_2, t_1) = \left\langle \hat{\mu} \exp\left[\frac{i}{\hbar}H_e t_1\right]\hat{\mu} \exp\left[\frac{i}{\hbar}H_g(t_2 + t_3)\right]\hat{\mu} \times \exp\left[-\frac{i}{\hbar}H_e t_3\right]\hat{\mu} \exp\left[-\frac{i}{\hbar}H_g(t_1 + t_2)\right]\rho_g \right\rangle \quad (5)$$

Here, $\hat{\mu}$ is an electronic dipole moment operator, $\rho_g = \sum_{i=1}^{N} a_n|g_n\rangle\langle g_n|$ is a ground-state nuclear density operator, with a_n as the population of the nth vibrational level $|g_n\rangle$ of the ground electronic state and N as the total number of initially populated ground vibrational states. The distribution of populations is Boltzmann, that is, $a_n = \exp(-\beta E_n)$, where $\beta = 1/kT$.

Assuming that pulses do not overlap, that is, t, τ_2, $\tau_1 > \tau$, (which is actually the necessary condition for deriving eq 3), we can set the lower limit for the integrals in eq 3 to $-\infty$. Using

a completeness relation $\sum |n\rangle\langle n| = 1$ in eqs 4 and 5 repeatedly, we obtain

$$R_2(t_3, t_2, t_1) = \sum_{n,k,u,v} \langle g_n|\hat{\mu}|e_u\rangle \times \exp\left[\frac{i}{\hbar}E_u^e(t_1 + t_2)\right]\langle e_u|\hat{\mu}|g_k\rangle\exp\left[\frac{i}{\hbar}E_k^g t_3\right]\langle g_k|\hat{\mu}|e_v\rangle \times \exp\left[-\frac{i}{\hbar}E_v^e(t_2 + t_3)\right]\langle e_v|\hat{\mu}|g_n\rangle\exp\left[-\frac{i}{\hbar}E_n^g t_1\right]\exp[-\beta E_n^g] \quad (6)$$

$$R_3(t_3, t_2, t_1) = \sum_{n,k,u,v} \langle g_n|\hat{\mu}|e_u\rangle\exp\left[\frac{i}{\hbar}E_u^e t_1\right]\langle e_u|\hat{\mu}|g_k\rangle \times \exp\left[\frac{i}{\hbar}E_k^g(t_2 + t_3)\right]\langle g_k|\hat{\mu}|e_v\rangle \times \exp\left[-\frac{i}{\hbar}E_v^e t_3\right]\langle e_v|\hat{\mu}|g_n\rangle \times \exp\left[-\frac{i}{\hbar}E_n^g(t_1 + t_2)\right]\exp[-\beta E_n^g] \quad (7)$$

By plugging eqs 6 and 7 into eq 3 and performing integrations, we get

$$P^{(3)}(t) = \left(\frac{i}{\hbar}\right)^3(\sqrt{2\pi}\tau E_0)^3 \sum_{n,k,u,v} e^{-\hbar\beta\varepsilon_n}\langle g_n|\hat{\mu}|e_u\rangle\langle e_u|\hat{\mu}|g_k\rangle \times \langle g_k|\hat{\mu}|e_v\rangle\langle e_v|\hat{\mu}|g_n\rangle \times e^{-(\varepsilon_k-\varepsilon_v)^2\tau^2/2}e^{-(\varepsilon_n-\varepsilon_u)^2\tau^2} \times e^{(\varepsilon_k-\varepsilon_n)(\varepsilon_u-\varepsilon_v)\tau^2} \times \{e^{i(\varepsilon_u-\varepsilon_v)\tau_2} + e^{i(\varepsilon_k-\varepsilon_n)\tau_2}\}e^{i(\varepsilon_k-\varepsilon_v)t}e^{i(\varepsilon_u-\varepsilon_n)\tau_1} \quad (8)$$

where we denote

$$\begin{aligned} \varepsilon_n &\equiv E_n^g/\hbar \\ \varepsilon_k &\equiv E_k^g/\hbar \\ \varepsilon_u &\equiv (E_u^e/\hbar) - (\omega_0 - \omega_{eg}) \\ \varepsilon_v &\equiv (E_v^e/\hbar) - (\omega_0 - \omega_{eg}) \end{aligned} \quad (9)$$

Here, $E_{\hbar}^g$ and $|g_n\rangle$ are the nth eigenvalue and the nth eigenstate of the Hamiltonian $\hat{H}_g$, respectively; E_v^e and $|e_v\rangle$ are the vth eigenvalue and the vth eigenstate of $\hat{H}_e$.

Matrix elements $\langle e_i|\hat{\mu}|g_j\rangle$ can be positive or negative depending on i and j. For systems with a chaotic classical limit, the distribution of matrix elements is shown to be Gaussian and centered at around zero.[26−28] We assume that near-symmetrical distribution of matrix elements around zero also holds for systems with regular dynamics; we illustrate this, in particular, in the Appendix on the example of a two-dimensional square-well potential. The result of summation (eq 8) is therefore determined by terms that contain squares of coefficients $\langle e_i|\hat{\mu}|g_j\rangle$, that is, by terms with $\{k = n, v \neq u\}$, $\{v = u, k \neq n\}$, and $\{k = n, v = u\}$. Let us consider these three cases separately, denoting contributions from each of them as $P_a^{(3)}(t)$, $P_b^{(3)}(t)$, and $P_c^{(3)}(t)$, respectively. The contribution from summation $\{k = n, v \neq u\}$ is

$$P_a^{(3)}(t) = \left(\frac{i}{\hbar}\right)^3(\sqrt{2\pi}\tau E_0)^3 \sum_{n=1}^{N} e^{-\hbar\beta\varepsilon_n} \sum_{u,v}{}' |\langle g_n|\hat{\mu}|e_v\rangle|^2|\langle g_n|\hat{\mu}|e_v\rangle|^2 \times e^{-(\varepsilon_n-\varepsilon_v)^2\tau^2/2}e^{-(\varepsilon_n-\varepsilon_u)^2\tau^2} \times \{e^{i(\varepsilon_u-\varepsilon_v)\tau_2} + 1\}e^{i(\varepsilon_n-\varepsilon_v)t}e^{i(\varepsilon_u-\varepsilon_n)\tau_1} \quad (10)$$

where $\sum'$ indicates the exclusion of terms with $u = v$.

In the Condon approximation, matrix elements $\langle g_n|\hat{\mu}|e_u\rangle$ can be represented as a product of an electronic dipole matrix element $\mu_0 \equiv \langle g|\hat{\mu}|e\rangle$, which is a constant, and a multidimensional Franck−Condon factor $S_{nu} \equiv \langle g, \nu_n|e, \nu_u\rangle$, which is an overlap between multidimensional nuclear wave functions. We now consider the question whether a multidimensional Franck−Condon factor S_{nu} can be considered as an independent random variable in summation over n and v, that is, independent of the difference of the corresponding eigenvalues $\varepsilon_n - \varepsilon_u$. In the case of chaotic motion, that was shown to be true;[28] for any given eigenstate $|g, \nu_n\rangle$, the Franck−Condon factor $\langle g, \nu_n|e, \nu_u\rangle$ is a Gaussian random variable, independent of eigenvalue. The reason is that an eigenstate of a classically chaotic system can be represented as a superposition of plane waves with random phase,[28] which is intrinsically independent of the eigenvalue, thus resulting in the random overlap integrals, that is, S_{nu}, independent of eigenvalues. In the case of regular motion, the independence of S_{nv} and $\varepsilon_n - \varepsilon_v$ is not obvious. In the Appendix, we consider an example of the simplest multidimensional regular system, a two-dimensional infinite square well, which allows analytical treatment. There, we show that the model of a square-well potential allows one to consider Franck−Condon factors as independent random variables. We therefore can assume similar independence of the Franck−Condon factors for the generic regular system. The independence of the Franck−Condon factors means that the summation (eq 10), which is an average $\sum^M ... = M\langle ...\rangle$, will result in the product of averages $\langle f(S_{ij})g(\varepsilon_i - \varepsilon_j)\rangle = \langle f(S_{ij})\rangle\langle g(\varepsilon_i - \varepsilon_j)\rangle$

$$P_a^{(3)}(t) = \left(\frac{i}{\hbar}\right)^3(\sqrt{2\pi}\tau E_0)^3\mu_0^2\langle S_{nu}^2 S_{nv}^2\rangle' \times \sum_{u,v}{}' \sum_{n=1}^{N} e^{-\hbar\varepsilon\beta_n}e^{-(\varepsilon_n-\varepsilon_v)^2\tau^2/2}e^{-(\varepsilon_n-\varepsilon_u)^2\tau^2} \times \{e^{i(\varepsilon_u-\varepsilon_v)\tau_2} + 1\}e^{i(\varepsilon_n-\varepsilon_v)t}e^{i(\varepsilon_u-\varepsilon_n)\tau_1} \quad (11)$$

where $\langle S_{nu}^2 S_{nv}^2\rangle'$ is the average of products of squared Franck−Condon factors for the vertical transitions from the N ground vibrational states, $u \neq v$.

The last summation over n in the above equation is the averaging of the expression under the summation sign over the different values of ε_n, $\sum_{n=1}^{N} ... = N\langle ...\rangle$. However, since ε_n is a random spectrum, its distribution density is known; it is a uniform distribution with the density $\rho(\varepsilon) = \hbar/N\langle\Delta E\rangle_0$, $0 < \varepsilon < N\langle\Delta E\rangle_0$, where $\langle\Delta E\rangle_0$ is the mean level spacing in the ground potential. Therefore $\sum_{n=1}^{N} ... = N(\hbar/N\langle\Delta E\rangle_0)\int d\varepsilon = (\hbar/\langle\Delta E\rangle_0)\int d\varepsilon$, and we can integrate ε_n out (setting the upper limit of integration to infinity because of the decay coefficient $\exp[-\hbar\beta\varepsilon]$) to have

$$P_a^{(3)}(t) = \left(\frac{i}{\hbar}\right)^3(\sqrt{2\pi}\tau E_0)^3\mu_0^2\langle S_{nu}^2 S_{nv}^2\rangle' \times \sqrt{\frac{\pi}{6}}\frac{\hbar}{\tau\langle\Delta E\rangle_0}e^{(\hbar\beta)^2/6\tau^2}e^{-[[(t-\tau_1)^2/6\tau^2]-i[\hbar\beta(t-\tau_1)/3\tau^2]]} \times \sum_v e^{-\hbar\beta\varepsilon_v}\sum_{r=\pm1,\pm2,...} e^{-[(\Delta_r^2\tau^2/3)-(2\hbar\beta\Delta_r/3)]}e^{(i\Delta_r/3)(2t+\tau_1)} \times \{e^{i\Delta_r\tau_2} + 1\} \times \left(1 + \mathrm{erf}\left[\frac{i(t - t_1) - \hbar\beta}{\sqrt{6\tau}} + \frac{2}{\sqrt{6}}\Delta_r\tau + \frac{3}{\sqrt{6}}\varepsilon_v\tau\right]\right) \quad (12)$$

where we have introduced a new variable $\Delta_r \equiv \Delta_{u-v} = \varepsilon_u - \varepsilon_v$, which stands for the distance between nearest r levels (rth

nearest-neighbor distance). We can neglect a nonconstant behavior of the error function (boundary effects) in the very small region $\varepsilon_v \in \{-2\pi/\tau, 2\pi/\tau\}$ and consider the error function in eq 12 as a step function, which equals 1 in the interval $\varepsilon_v \in \{0,\infty\}$ and 0 outside. Equation 12 thus takes the form

$$P_a^{(3)}(t) = \left(\frac{i}{\hbar}\right)^3 (\sqrt{2\pi}\tau E_0)^3 \mu_0^2 \langle S_{nu}^2 S_{nv}^2\rangle' \times \sqrt{\frac{\pi}{6}}\frac{\hbar}{\tau\langle\Delta E\rangle_0} e^{(\hbar\beta)^2/6\tau^2} e^{-[[(t-\tau_1)^2/6\tau^2]-i[\hbar\beta(t-\tau_1)/3\tau^2]]} \times 2\sum_{v=0}^{\infty} e^{-\hbar\beta\varepsilon_v} \sum_{r=\pm1,\pm2,\ldots} e^{-[(\Delta_r^2\tau^2/3)-(2\hbar\beta\Delta_r/3)]} e^{(i\Delta_r/3)(2t+\tau_1)} \times \{e^{i\Delta_r\tau_2} + 1\} \quad (13)$$

Again, the summation over v is an averaging over the variable ε_v. The position in spectrum ε_v and the distance to its nearest neighbor $\Delta_r(v)$ are independent variables and therefore can be averaged out separately. This results in

$$P_a^{(3)}(t) = \left(\frac{i}{\hbar}\right)^3 (\sqrt{2\pi}\tau E_0)^3 \mu_0^2 \langle S_{nu}^2 S_{nv}^2\rangle' \times \sqrt{\frac{\pi}{6}}\frac{\hbar}{\tau\langle\Delta E\rangle_0} e^{(\hbar\beta)^2/6\tau^2} e^{[-[(t-\tau_1)^2/6\tau^2]-i[\hbar\beta(t-\tau_1)/3\tau^2]]} \times 2(\sum_{v=0}^{\infty} e^{-\hbar\beta\varepsilon_v}) \times \sum_{r=\pm1,\pm2,\ldots} \langle e^{[-(\Delta_r^2\tau^2/3)-(2\hbar\beta\Delta_r/3)]} e^{(i\Delta_r/3)(2t+\tau_1)} \times \langle\{e^{i\Delta_r\tau_2} + 1\}\rangle \quad (14)$$

where the last averaging is due to the summation over v. Since Δ_r has different values at different parts of spectrum, then the averaging over v results in the average over Δ_r. The latter can be done using nearest-neighbor distribution functions, which are known functions for both Poisson and GOE statistics.[15] Thus, we have

$$\sum_{r=\pm1,\pm2,\ldots} \langle e^{-[(\Delta_r^2\tau^2/3)-(2\hbar\beta\Delta_r/3)]} e^{(i\Delta_r/3)(2t+\tau_1)}\{e^{i\Delta_r\tau_2} + 1\}\rangle = 2\int_0^{\infty} e^{-[(\Delta^2\tau^2/3)-(2\hbar\beta\Delta_r/3)]}\left\{\cos\left[\Delta\left(\frac{2t+\tau_1}{3} + \tau_2\right)\right] + \cos\left[\Delta\left(\frac{2t+\tau_1}{3}\right)\right]\right\} \times \sum_{r=1,2,\ldots} \rho_r(\Delta)d\Delta \quad (15)$$

One can see that the statistics energy spectrum enters the above expression as a sum $\rho(\Delta) = \sum_r \rho_r(\Delta)$, which is just a two-level density of states.[29] For now, we postpone a further consideration of the expression in eq 15 until the next section and continue with the remaining contributions $P_b^{(3)}(t)$ and $P_c^{(3)}(t)$. Denoting the expression in eq 15 with $F(t)$, we get the final expression for $P_a^{(3)}(t)$ in the form of

$$P_a^{(3)}(t) = Ce^{-[[(t-\tau_1)^2/6\tau^2]-i[\hbar\beta(t-\tau_1)/3\tau^2]]}F(t) \quad (16)$$

where $C = (i/\hbar)^3[(2\pi)^{1/2}\tau E_0)^3\mu_0^2\langle S_{nu}^2 S_{nv}^2\rangle'(\pi/6)^{1/2}[2\hbar/\tau\langle\Delta E\rangle_0][1/\beta\langle\Delta E\rangle]e^{(\hbar\beta)^2/6\tau^2}$ is a constant and where we have used $\sum_{v=0}^{\infty} e^{-\hbar\beta\varepsilon_v} \approx 1/\beta\langle\Delta E\rangle$ with $\langle\Delta E\rangle$ being the mean level spacing in the excited electronic potential surface.

Let us now consider $P_b^{(3)}(t)$; it reads

$$P_b^{(3)}(t) = \left(\frac{i}{\hbar}\right)^3 (\sqrt{2\pi}\tau E_0)^3 \sum_{n=1}^{N} e^{-\hbar\beta\varepsilon_n} \sum_{k,v} |\langle g_n|\hat{\mu}|e_v\rangle|^2 |\langle g_k|\hat{\mu}|e_v\rangle|^2 \times e^{-(\varepsilon_k-\varepsilon_v)^2\tau^2/2} e^{-(\varepsilon_n-\varepsilon_v)^2\tau^2} \times \{1 + e^{i(\varepsilon_k-\varepsilon_n)\tau_2}\} e^{i(\varepsilon_k-\varepsilon_v)t} e^{i(\varepsilon_v-\varepsilon_n)\tau_1} \quad (17)$$

Using the same assumptions as those in the derivation of $P_a^{(3)}(t)$ and replacing summations $\sum_{n=1}^{N}$ and $\sum_{k=1}^{\infty}$ with the integral $(\hbar/\langle\Delta E\rangle_0)\int_0^{\infty} d\varepsilon$, we get

$$P_b^{(3)}(t) = C' e^{-[[2t^2+\tau_1^2/4\tau^2]+i(\hbar\beta\tau_1/2\tau^2)]} \times \left(1 + e^{-[\tau_2(4t+2\tau_1+3\tau_2)/4\tau^2]+i(\hbar\beta\tau_2/2\tau^2)]}\right) \quad (18)$$

where $C' = (i/\hbar)^3[(2\pi)^{1/2}\tau E_0)^3\mu_0^2\langle S_{nu}^2 S_{kv}^2\rangle'\pi(2)^{1/2}[(\hbar/\tau\langle\Delta E\rangle_0)^2][1/\beta\langle\Delta E\rangle]e^{(\hbar\beta)^2/4\tau^2}$. Obviously, the contribution of this term to the overall nonlinear polarization is negligible when the conditions of pulse nonoverlapping t, τ_1, $\tau_2 > \tau$ are satisfied.

The last term to consider is $P_c^{(3)}(t)$

$$P_c^{(3)}(t) = 2\left(\frac{i}{\hbar}\right)^3 (\sqrt{2\pi}\tau E_0)^3 \sum_{n=1}^{N} e^{-\hbar\beta\varepsilon_n} \sum_{v} |\langle g_n|\hat{\mu}|e_v\rangle|^4 \times e^{-(3\tau^2/2)(\varepsilon_n-\varepsilon_v)^2} e^{i(\varepsilon_n-\varepsilon_v)(t-\tau_1)} \quad (19)$$

which simplifies to

$$P_c^{(3)}(t) = 2C\frac{\langle S_{nv}^4\rangle}{\langle S_{nu}^2 S_{nv}^2\rangle'} e^{-[[(t-\tau_1)^2/6\tau^2]-i[\hbar\beta(t-\tau_1)/3\tau^2]]} \quad (20)$$

The overall third-order nonlinear polarization reads

$$P^{(3)}(t) = P_a^{(3)}(t) + P_b^{(3)}(t) + P_c^{(3)}(t) = Ce^{-[[(t-\tau_1)^2/6\tau^2]-i[\hbar\beta(t-\tau_1)/3\tau^2]]}\left(F(t) + 2\frac{\langle S_{nv}^4\rangle}{\langle S_{nu}^2 S_{nv}^2\rangle'}\right) + P_b^{(3)}(t) \quad (21)$$

Here, we did not substitute for a small contribution of $P_b^{(3)}(t)$ in order not to overload the formula. One can see that at $t = \tau_1$, we have an echo.

III. $F(t)$ for Two Types of Statistics

Obviously, $F(t)$ carries the information about level statistics in the excited electronic state. We now consider the two cases of statistics separately.

A. Poisson Statistics. Systems with regular dynamics possess Poisson nearest-neighbor energy level statistics. For this statistics, energy levels are uncorrelated, and the two-level density of states is uniform

$$\rho(\omega) = \sum_{r=1,2,\ldots}^{\infty} \rho_r(\omega) = \frac{1}{\langle\Delta E\rangle/\hbar} \quad (22)$$

where $\langle\Delta E\rangle$ is a mean level spacing. Thus, $F(t)$ for systems with regular dynamics reads

$$F(t) = 2\left\{g_{\tilde{\alpha}\tilde{\beta}}\left(\frac{2t + \tau_1 + 3\tau_2}{3\tau}\right) + g_{\tilde{\alpha}\tilde{\beta}}\left(\frac{2t + \tau_1}{3\tau}\right)\right\} \quad (23)$$

where

$$g_{\tilde{\alpha}\tilde{\beta}}(x) = \mathrm{Re}\left\{\frac{\sqrt{3\pi}}{\tilde{\alpha}} e^{-(3/4)(x+i(2\tilde{\beta}/3))^2} \times \left(1 + i\,\mathrm{erfi}\left[\frac{\sqrt{3}}{2}(x + i(2\tilde{\beta}/3))\right]\right)\right\} \quad (24)$$

Here, we have introduced dimensionless parameters $\tilde{\alpha} = \tau\langle\Delta E\rangle/\hbar$ and $\tilde{\beta} = \beta\hbar/\tau$. The necessary conditions for the photon-echo experiment described in this paper look very simple in terms of these parameters; they are

$$\begin{aligned} &\tilde{\alpha} < 1 \\ &\tilde{\alpha}\tilde{\beta} \ll 1 \end{aligned} \quad (25)$$

The first condition means that the spectral width of the laser pulse should be greater than the mean level spacing in order to excite at least two states to form an excited superposition state, as discussed in the Introduction. The second condition in eq 25, which is $\beta\langle\Delta E\rangle \ll 1$, defines the obvious requirement for the allowed temperature; it should be greater than the mean level spacing to populate several levels to form a statistics of levels.

A photon-echo signal measured in experiments is given by[25]

$$\chi(\tau_1, \tau_2) = \int_0^\infty |P(t)|^2\, dt \quad (26)$$

Substituting eqs 21 and 23 into the above integral results in monotonically decaying signals shown in Figure 3a,b.

B. GOE Statistics. For GOE statistics, the first nearest-neighbor distribution function is given by the Wigner distribution[15]

$$\rho_1(\omega) = \frac{\pi}{2}\frac{\omega\hbar}{\langle\Delta E\rangle}\frac{\hbar\exp\{-(\pi/4)[\langle\omega\hbar/\langle\Delta E\rangle\rangle]^2\}}{\langle\Delta E\rangle} \quad (27)$$

where $\langle\Delta E\rangle$ is a mean level spacing. In this case, the two-level density of states reads[29]

$$\rho(\omega) = \frac{\hbar}{\langle\Delta E\rangle}\left(1 - c^2(\omega) - \frac{dc(\omega)}{d\omega}\int_\omega^\infty c(\omega')d\omega'\right) \quad (28)$$

with $c(\omega) = \sin[\pi\hbar\omega/\langle\Delta E\rangle]/(\pi\hbar\omega/\langle\Delta E\rangle)$. Numerical integration of eq 15 with eq 28 gives

$$F(t) = 2\left\{f_{\tilde{\alpha}\tilde{\beta}}\left(\frac{2t + \tau_1 + 3\tau_2}{3\tau}\right) + f_{\tilde{\alpha}\tilde{\beta}}\left(\frac{2t + \tau_1}{3\tau}\right)\right\} \quad (29)$$

where functions $f_{\tilde{\alpha}\tilde{\beta}}$ in the range of parameters given by eq 25 can be well-approximated by analytic functions

The plots of $f_{\tilde{\alpha}\tilde{\beta}}(x)$ and $g_{\tilde{\alpha}\tilde{\beta}}(x)$ are shown in Figure 4 for different temperatures. One can see that $f_{\tilde{\alpha}\tilde{\beta}}(x)$ has a clear minimum. Its

$$f_{\tilde{\alpha}\tilde{\beta}}(x) = g_{\tilde{\alpha}\tilde{\beta}}(x) - \frac{8}{\pi}\mathrm{Re}\left[\frac{\mathrm{erf}^2[(\tilde{\alpha}x + i(2\tilde{\alpha}\tilde{\beta}/3))/3]}{(\tilde{\alpha}x + i(2\tilde{\alpha}\tilde{\beta}/3))^2}\right] \quad (30)$$

position is a nonlinear function of parameters $\tilde{\alpha}$ and $\tilde{\beta}$, which can be found numerically; in the range of $\tilde{\beta} < 0.3$, $0.4 < \tilde{\alpha} < 1$, it can be given by the approximate formula $x_{\min} = 1.25(\tilde{\beta}/\tilde{\alpha}^{1.39}) + (2.61/\tilde{\alpha}^{0.2}) \approx 2.61/\tilde{\alpha}^{0.2}$. $F(t)$ for the echo condition $t = \tau_1$ thus has the minimum at $t \sim 2.6\tau^{0.8}$.

Straightforward numerical calculation of the summation in eq 11 was also performed to check the obtained analytical results. For the energy spectrum ε_n, 400 levels with the mean level spacing of $\langle\Delta E\rangle = 1$ were randomly generated on the interval $(0, 400\langle\Delta E\rangle)$ using a uniform distribution function. For the energy spectrum $\varepsilon_{v,u}$, in the case of regular motion, the same generation of the spectrum as that above was used. In the case of chaotic motion, 400 level spacings $\{\Delta_i\}$ were generated using the Metropolis algorithm with the Wigner distribution function (eq 27) and $\langle\Delta E\rangle = 1$; the spectrum ε_v was then obtained as $\varepsilon_v = \sum_{i=1}^{v}\Delta_i$. The result of the summation in eq 11 is given in Figure 5 as a function of t for $\tau = 0.5$, $\tau_1 = t$ (echo condition), and different values of the inverse temperature β and τ_2. The variation of τ_2 does not significantly affect the position of the minimum of $F(t)$; yet, it helps to average out the fluctuations of the numerical results due to a limited number of spectral lines, which may effectively become even smaller at lower temperatures. One can see that for the Wigner nearest-neighbor distribution, $F(t)$ in Figure 5 has a minimum at $t = 2.6\tau^{0.8} = 1.5$, in accordance with the analytical predictions.

Calculation of a signal (eq 26) with eqs 29 and 30 is shown in Figure 3c,d. The $\chi(\tau_1, \tau_2)$ has a minimum at $\tau_1 \sim 4\tau$ for any given value of τ_2, and its location along τ_1 axis is independent of τ_2. We call this minimum a suppression of photon-echo signal.

IV. Mixed Spectral Statistics

It is interesting that the minimum of the photon-echo signal at $\tau_1 \approx 4\tau$ is not sensitive to the purity of the GOE spectral statistics or the type of correlated level statistics. The level statistics enters the expression for the photon-echo signal (eq 21) as a two-level correlation function $\rho(\omega)$. In some sense, the minimum of the photon-echo signal is directly related to the dip in $\rho(\omega)$ at $\omega = 0$. As long as $\rho(\omega)$ is different from the uniform distribution of completely uncorrelated levels (eq 22), there will be a minimum in the photon-echo signal. For instance, if the spectrum is a mixture of the correlated and the uncorrelated levels, its nearest-neighbor statistics can be described with a Brody distribution, which is an intermediate between the Poisson and the Wigner distributions. The two-level correlation functions will look then as an intermediate between the expressions in eqs 22 and 28. As an example, the two-level density of states shown in the inset of Figure 6 results in the function $F(t)$ shown in Figure 6. One can see that $F(t)$ still has a clear minimum in the region of $\sim 4\tau$. The depth of the minimum is proportional to the strength of the spectral correlation.

Interestingly, the type of the spectral level statistics in the ground electronic state is not important. In the present analysis, we have made an assumption about the random level statistics in the ground electronic state for easier analytical derivations, yet as one can see, the spectroscopic signal, and in particular its minimum, depends only on the term $P_{\bar{a}}^{(3)}(t)$, which includes only the differences between energy levels ε_u and ε_v in the excited electronic state and therefore effectively probes only the level statistics of the excited electronic state. We will publish the results on the general level statistics elsewhere.

V. Results and Discussion

The main result of the present analysis is that the photon-echo experiment carried out with the conditions in eq 25 should

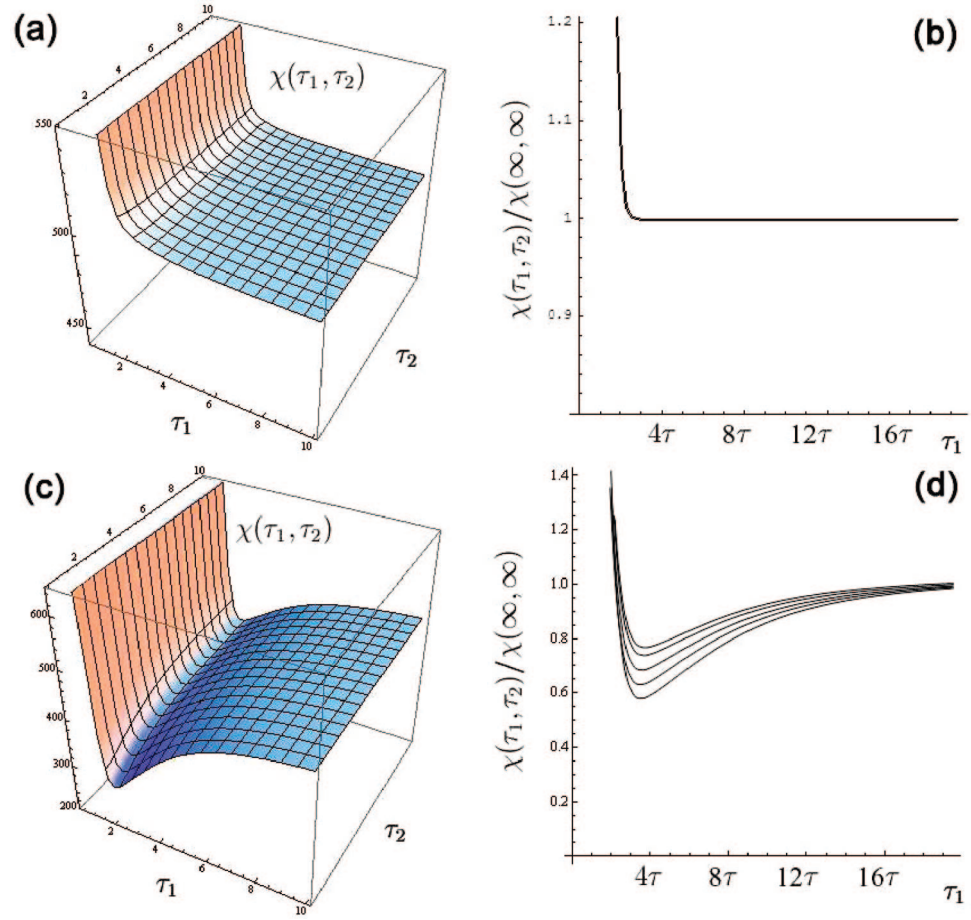

Figure 3. Photon-echo signals for regular systems (a,b) and irregular systems (c,d) at a temperature of $\beta\langle\Delta E\rangle = 0.05$. Inset (d) contains plots for increasing values of τ_2 from the bottom curve to the top curve; $\tau_2 = \tau$, 5τ, 10τ, 20τ, ∞. The values of the parameters are $\langle\Delta E\rangle = 1$, $\tau = 0.5$, and $\hbar = 1$.

result in the suppression of echo-signals at $\tau_1 \sim 4\tau$ for chaotic systems, where τ is a pulse duration. The time interval between second and third laser pulses, τ_2, does not influence the location of the signal's minimum along the τ_1 axis. The suppression can be considerable; the general formula for the ratio $\chi(\tau_1,\tau_2)/\chi(\infty,\infty)$ near the global minimum $\tau_1 = 4\tau$ and $\tau_2 = 0$ at high temperatures, $\beta\langle\Delta E\rangle \ll 1$, is

$$\frac{\chi(4\tau,0)}{\chi(\infty,\infty)} \approx \left|1 - \frac{8}{\pi}\frac{\langle S_{n\mu}^2 S_{n\nu}^2\rangle'}{\langle S_{n\nu}^4\rangle}\left[2\frac{\mathrm{erf}^2\left(\frac{4\tau}{3}\right)}{(4\tau)^2}\right]\right|^2 \qquad (31)$$

where τ has dimensionless units of $\hbar/\langle\Delta E\rangle$. We can estimate the ratio assuming $|S_{n\mu}|$ and $|S_{n\nu}|$ are uncorrelated, uniformly distributed variables; then, $\langle S_{n\mu}^2 S_{n\nu}^2\rangle'/\langle S_{n\nu}^4\rangle = \langle S^2\rangle\langle S^2\rangle/\langle S^4\rangle = 5/9$, which results in $[\chi(4\tau,0)/\chi(\infty,\infty)] \to 0.36$ and $\tau \to 0$. Thus, the suppression of the photon-echo signal can be up to 50%.

On the other hand, the photon-echo signal of regular systems $\chi(\tau_1, \tau_2)$ does not have any minima (Figures 3a,b). Thus, the following conditions always hold: $\chi(4\tau,\tau_2)/\chi(\infty,\infty) \geq 1$ for regular systems and $\chi(4\tau,\tau_2)/\chi(\infty,\infty) < 1$ for irregular systems. In real experiments, $\chi(\tau_1,\tau_2)$ decays to zero due to different broadening mechanisms, but on the time scale of an ultrafast experiment, we can neglect broadening effects and thus consider the long time limit of $\chi(\tau_1,\tau_2)$ as a constant, which we plot in Figure 3 as $\chi(\infty,\infty)$. Since the location of the correlation minimum at $\tau_1 = 4\tau$ does not depend on τ_2 (Figure 3d), we can

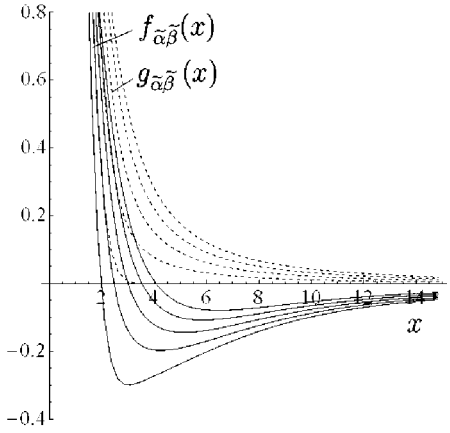

Figure 4. The functions $f_{\tilde{\alpha}\tilde{\beta}}(x)$ (solid line) and $g_{\tilde{\alpha}\tilde{\beta}}(x)$ (dashed line) for the different values of the inverse temperature $\beta = 1/kT$. The values of the parameters are $\tilde{\alpha} = 0.5$, $\tilde{\beta} = 2\beta$, $\tau = 0.5$, and $\hbar = 1$. The values of β change from 0 (the bottom solid and dashed plots) to 0.8 (the top solid and dashed plots).

make the above inequalities stronger by averaging over some interval of τ_2. The latter averaging can remove experimental nonideality and thus provide more conclusive measurements.

The physics of the observed suppression of the echo signal is similar to the physics for the suppression of the averaged survival probability $|\langle\psi(0)|\psi(t)\rangle|^2$ discussed in refs 14 and 15. The main idea is that since the energy levels obeying GOE statistics are correlated on the energy scale $\langle\Delta E\rangle$, the superposition state $|\psi(t)\rangle = \sum \exp(-iE_n t/\hbar)|n\rangle$ would remember its initial

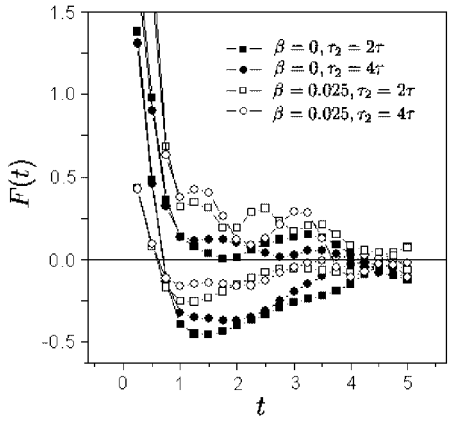

Figure 5. The results of the numerical calculation of $F(t)$ by evaluating the summations in eq 11. The top four curves correspond to the Poisson nearest-neighbor statistics; the bottom four curves correspond to the GOE nearest-neighbor statistics. Solid symbols correspond to $\beta = 0$, and open symbols correspond to $\beta\langle\Delta E\rangle = 0.025$. Squares (open and solid) represent the results for $\tau_2 = 2\tau$, and circles (open and solid) represent the results for $\tau_2 = 4\tau$. The other parameters are $\langle\Delta E\rangle = 1$, $\tau = 0.5$, and $\hbar = 1$.

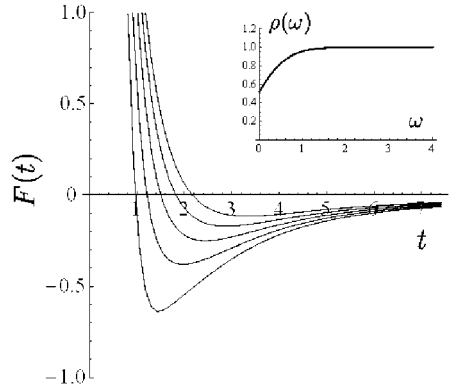

Figure 6. $F(t)$ for the two-level density of weakly correlated states $\rho(\omega)$ shown in the inset. The magnitudes of the parameters are $\tau = 0.5$, $\langle\Delta E\rangle = 1$, and $\hbar = 1$.

conditions on the time scale of $\Delta t = \hbar/\langle\Delta E\rangle$. This time scale defines the interval of quantum coherence, which will "survive" after the averaging over initial conditions and energy level statistics. During this time, $|\langle\psi(0)|\psi(t)\rangle|^2$ would behave as a typical quantum dephasing process with oscillatory behavior around its average value due to quantum coherence effects. As a result, $|\langle\psi(0)|\psi(t)\rangle|^2$ can go below its long time limit (it could have made several oscillations around its long time limit; however, the time of coherence Δt ends up earlier than the second oscillation). For the regular motion, however, the energy levels do not have any correlation, and thus, no time interval Δt of quantum coherence exists after the averaging over the ensemble of levels. Therefore, $|\psi(t)\rangle$ is not correlated with its initial conditions and decays to its statistical average.

In the proposed experiment, the time domain signature of chaotic motion at 4τ arises from the minimum of the integrated signal and not from the response function itself. Although the response function is more fundamental since it is invariant under experimental conditions, only its convolution with the electric field yields the results of the present theory. The reason lies in a particular physical mechanism in which we are interested. Each eigenstate in the ground potential surface being irradiated by a laser pulse forms a superposition state in the excited electronic potential surface. It is the time evolution of a superposition state (when averaged over many mutually incoherent superposition states) that reveals energy level statistics in the excited electronic potential surface. To form a superposition state, we need an explicit presence of a shaped laser field in our theory. Since the information about level statistics is determined by a superposition state and the latter is determined by the parameters of a laser pulse, the information on level statistics should be determined by the parameters of the laser pulse. This is exactly what we have in our theory; the minimum of the photon-echo signal is located at approximately four pulse durations. The total number of the excited eigenstates N_e in the excited electronic potential is equal to the number of initially populated eigenstates N_g in the ground electronic potential multiplied by the ratio of the mean level spacings in the ground electronic potential and that in the excited electronic potential, $N_e = N_g\langle\Delta E\rangle_0/\langle\Delta E\rangle$. To have good statistics, we need to populate a considerable number of ground states $N_g \gg 1$, which suggests performing the experiment at high temperatures, that is, $\beta\langle\Delta E\rangle_0 \ll 1$.

VI. Conclusions

In this paper, we have shown that information about level statistics can be extracted from a time domain signal of the photon-echo experiment. Correlated (GOE) statistics of level spacings results in a suppressed photon-echo signal at $\tau_1 = 4\tau$, whereas Poisson level statistics does not show a dip in the intensity of a signal. The main advantage of the proposed experiment is the implication of a nonlinear photon-echo technique which may overcome both homogeneous and inhomogeneous energy level broadening. The possibility to conduct the experiment for thermal ensembles makes it easy for practical applications.

Acknowledgment. We thank the anonymous reviewers for their valuable comments and suggestions and professor Bob Field for stimulating discussions. The research reported here is supported by Camille & Henry Dreyfus Foundation and by the U.S. Army through the Institute of Soldier Nanotechnologies at MIT.

Appendix

In this appendix, we consider the simplest case of a multidimensional anharmonic system with regular dynamics, a two-dimensional infinite square-well potential, $-L_x/2 < x < L_x/2$ and $-L_y/2 < y < L_y/2$. Its eigenstates and eigenvalues are known to be

$$\Psi_{n_x,n_y} = \sqrt{\frac{4}{L_x L_y}}\sin\left[\frac{\pi n_x(x - L_x/2)}{L_x}\right]\sin\left[\frac{\pi n_y(y - L_y/2)}{L_y}\right]$$
$$E_{n_x,n_y} = \frac{\pi^2\hbar^2}{2m}\left[\left(\frac{n_x}{L_x}\right)^2 + \left(\frac{n_y}{L_y}\right)^2\right] \quad (32)$$

For the irrational ratio of L_x and L_y, the simple quadratic spectrum (eq 32) forms a random spectrum and results in a Poisson nearest-neighbor distribution. In the present analysis, we took $L_x = 2^{1/8}L_y$ since it yields a Poisson distribution for the first 100 levels.

In application to the two-electronic-state problem considered in the present paper, we represent the ground electronic potential surface as a two-dimensional square well and the excited electronic surface with a two-dimensional square well twice the size, $L_{x'} = 2L_x$ and $L_{y'} = 2L_y$; see Figure 7. We numerate energy levels $E_i \equiv E_{n_x,n_y}$, $i = 1, 2, 3,...$ in the ground well and $E_{j'} \equiv E_{n_{\acute{x}},n_{\acute{y}}}$, $j = 1, 2, 3,...$ in the upper well in ascending order. The

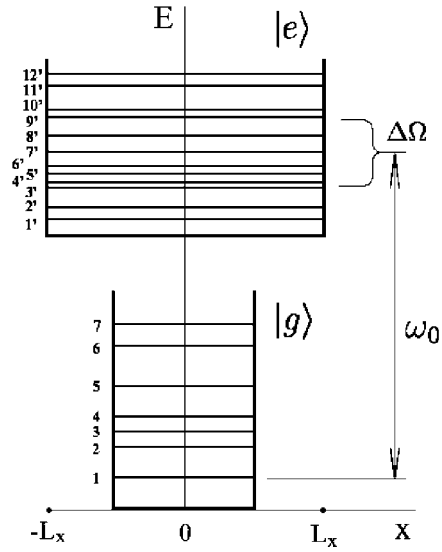

Figure 7. The model of a two-electronic-state system with two-dimensional square-well potential surfaces. Only one dimension, x, is shown in the figure. Numbers along the vertical axis numerate energy levels. A laser pulse with a spectral width of $\Delta\Omega$ and a frequency of ω_0 excites energy states $E_{n_x',n_y'}$, which are in the range of $E_{n_x,n_y} + \hbar\omega_0 \pm \hbar\Delta\Omega/2$.

Franck−Condon factors S_{ij} of the overlap of states Ψ_{n_x,n_y} and $\Psi_{n_x',n_y'}$ that correspond to the two eigenvalues E_i and $E_{j'}$, respectively, are

$$S_{ij} = 2s(n_x, n_x')s(n_y, n_y') \tag{33}$$

where

$$s(n,n') = \begin{cases} \frac{1}{2}\cos\left(\frac{\pi n}{2}\right) & \text{if } n' = 2n \\ \frac{4n(\sin(\pi n'/4) - \cos(\pi n)\sin(3\pi n'/4))}{\pi(4n^2 - n'^2)} & \text{if } n' \neq 2n \end{cases} \tag{34}$$

If initially an ith eigenstate with an eigenvalue E_i is populated in the ground potential well, a laser pulse with a spectral width $\Delta\Omega$ and frequency ω_0 will excite eigenstates in the upper potential well with eigenvalues E_j' that fit into the energy range of $E_i + \hbar\omega_0 \pm \hbar\Delta\Omega/2$; see Figure 7. We can thus predict all of the Franck−Condon factors S_{ij} which are involved in the excitation from the state $|i\rangle$; there will be, on average, $\hbar\Delta\Omega/\langle\Delta E'\rangle$ of them, where $\langle\Delta E'\rangle$ is the mean level spacing in the upper potential well. In numerical analysis, we used $L_x = 1$, $\pi^2\hbar^2/2m = 1$, $\langle\Delta E\rangle = 1.8$, $\langle\Delta E'\rangle = 0.45$, and $\Delta\Omega = 4$, and the difference between $\hbar\omega_0$ and the energy gap between the bottoms of potential wells is equal to 10. The Franck−Condon factors involved in the process of excitation from the first 200 states of the ground potential well are shown in Figure 8. Only the overlap integrals between the states which have eigenvalues within the spectral window $\Delta\Omega$ of the laser pulse are considered. From Figure 8a,c, one can see that there is no correlation between the eigenvalues, or indices i and j, and the values of the Franck−Condon factors S_{ij}. Figure 8c also shows that, for the considered square-well model, the values of the overlap integrals are symmetrically distributed around zero. We thus can consider eigenvalues and Franck−Condon factors to be uncorrelated.

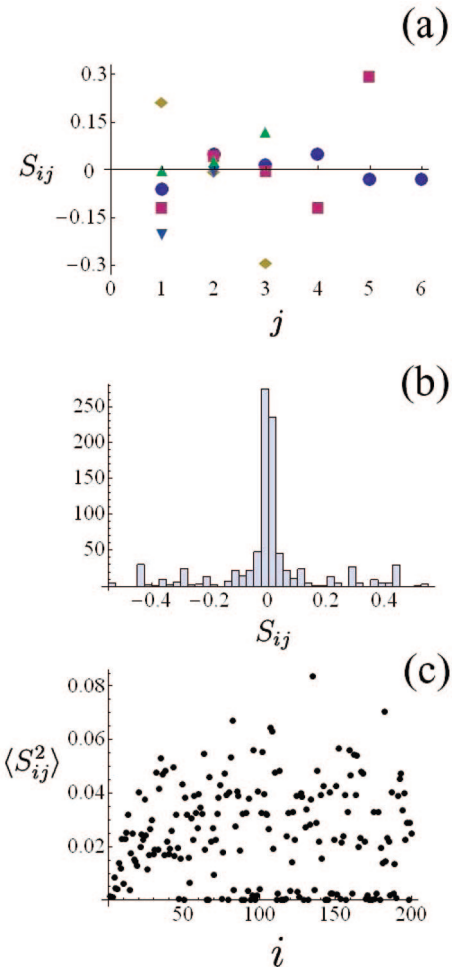

Figure 8. Franck−Condon factors S_{ij} for the pair of ground and excited two-dimensional infinite square-well potentials. (a) The overlap integral between the ith eigenfunction of the ground potential well and the jth eigenfunction of the upper potential well; circles correspond to $i = 1$, squares to $i = 46$, diamonds to $i = 91$, up-triangles to $i = 136$, and down-triangles to $i = 181$; only those j's with the corresponding eigenvalues that fit into the laser pulse's spectral window are presented (the integer numbers along the j-axis do not correspond to the actual values of j but only count the number of j states that fit into the spectral window). (b) The occurrence frequencies of the values of the overlap integrals S_{ij} for the first 200 eigenstates of the ground well (the upper eigenstates are picked as in case (a)). (c) The dependence of the mean square of the Franck−Condon factor averaged over the possible values of j, that is, over the eigestates of the upper potential which overlaps with the eigenstates of the ground potential, as discribed in case (a), as a function of the ground potential eigenstate i.

References and Notes

(1) Berry, M. V.; Tabor, M. *Proc. R. Soc. London, Ser. A* **1977**, *356*, 375.

(2) Lombardi, M.; Labastie, P.; Bordas, M. C.; Broyer, M. *Ber. Bunsen-Ges. Phys. Chem.* **1988**, *92*, 387.

(3) Lombardi, M.; Labastie, P.; Bordas, M. C.; Broyer, M. *J. Chem. Phys.* **1988**, *89*, 3479.

(4) Haller, E.; Koppel, H.; Cederbaum, L. S. *Phys. Rev. Lett.* **1984**, *52*, 1665.

(5) Seligman, T. H.; Verbaarschot, J. J. M.; Zirnbauer, M. R. *Phys. Rev. Lett.* **1984**, *53*, 215.

(6) Sunberg, R. L.; Abramson, E.; Kinsey, J. L.; Field, R. W. *J. Chem. Phys.* **1985**, *83*, 466.

(7) Chen, Y.; Hallet, S.; Jonas, D. M.; Kinsey, J. L.; Field, R. W. *J. Opt. Soc. Am. B* **1990**, *7*, 1805.

(8) Delon, A.; Jost, R.; Lombardi, M. *J. Chem. Phys.* **1991**, *95*, 5701.

(9) Michaille, L.; Pique, J. P. *Phys. Rev. Lett.* **1998**, *82*, 2083.
(10) Abramson, E.; Field, R. W.; Innes, D. I.; Kinsey, J. L. *J. Chem. Phys.* **1983**, *80*, 2298.
(11) Michaille, L.; Pique, J. P. *Phys. Rev. Lett.* **1998**, *82*, 2083.
(12) Bohigas, O.; Giannoni, M. J.; Schmitt, C. *Phys. Rev. Lett.* **1984**, *52*, 1.
(13) Nakamura, H.; Kato, S. *Chem. Phys. Lett.* **1998**, *297*, 187.
(14) Pechukas, P. *J. Phys. Chem.* **1984**, *88*, 4823.
(15) Wilkie, J.; Brumer, P. *J. Chem. Phys.* **1997**, *107*, 4893.
(16) Wilkie, J.; Brumer, P. *Phys. Rev. Lett.* **1991**, *67*, 1185.
(17) Mukamel, S.; Khidekel, V.; Chernyak, V. *Phys. Rev. E* **1996**, *53*, R1.
(18) Wu, J.; Cao, J. *J. Chem. Phys.* **2001**, *115*, 5381.
(19) Noid, W. G.; Ezra, G. S.; Loring, R. *J. Phys. Chem.* **2004**, *108*, 6563.
(20) Noid, W. G.; Loring, R. *J. Chem. Phys.* **2005**, *122*, 174507.
(21) Kryvohuz, M.; Cao, J. *Phys. Rev. Lett.* **2005**, *95*, 180405.
(22) Kryvohuz, M.; Cao, J. *Phys. Rev. Lett.* **2006**, *96*, 030403.
(23) Malinin, S. V.; Chernyak, V. Y. *Phys. Rev. E.* **2008**.
(24) Malinin, S. V.; Chernyak, V. Y. *Phys. Rev. E.* **2008**.
(25) Mukamel, S. *The Principles of Nonlinear Optical Spectroscopy*; Oxford: London, 1995.
(26) Berry, M. V. *J. Phys. A* **1977**, *10*, 2083.
(27) Austin, E. J.; Wilkinson, M. *Europhys. Lett.* **1992**, *20*, 589.
(28) Stechel, E. B.; Heller, E. J. *Annu. Rev. Phys. Chem.* **1984**, *35*, 563.
(29) Mehta, M. L. *Random Matrices*; Academic: New York, **1991**.

JP804604H